

# A Theory of Pattern Recognition for the Discrimination between Muon and Electron in the Super-Kamiokande

V.I. Galkin<sup>1</sup>, A.M. Anokhina<sup>1</sup>, E. Konishi<sup>2</sup>, and A. Misaki<sup>3</sup>

<sup>1</sup> Department of Physics, Moscow State University, Moscow, 119992, Russia

<sup>2</sup> Graduated School of Science and Technology, Hirosaki University, 036-8561, Hirosaki, Japan

<sup>3</sup> Advanced Research Institute for Science and Engineering, Waseda University, 169-0092, Tokyo, Japan  
e-mail: misaki@kurenai.waseda.jp

Received: date / Revised version: date

**Abstract.** The standard Super-Kamiokande analysis uses an estimator for particle identification by which it discriminates  $e$  ( $\nu_e$ ) from  $\mu$  ( $\nu_\mu$ ). Use of this estimator has led to the claim of a significant deficiency of  $\mu$  ( $\nu_\mu$ ), suggesting the existence of neutrino oscillations. We investigate three areas of concern for the Super-Kamiokande estimator: the separation of the spatial part from the angular part in the probability functions, the neglect of fluctuations in the Cherenkov light in different physical processes due to the charged particles concerned, and the point-like approximation for the emission of Cherenkov light. We show that the first two factors are important for the consideration of stochastic processes in the generation of the Cherenkov light, and that the point-like assumption oversimplifies the estimation of the Cherenkov light quantities. We develop a new discrimination procedure for separating electron neutrinos from muon neutrinos, based on detailed simulations carried out with GEANT 3.21 and with newly derived mean angular distribution functions for the charged particles concerned (muons and electrons/positrons), as well as the corresponding functions for the relative fluctuations. These angular distribution functions are constructed introducing a “moving point” approximation. The application of our procedure between the discrimination between electron and muon to the analysis of the experimental data in SK will be made in a subsequent paper.

**PACS.** 13.15.+g Neutrino interactions – 14.60.-z leptons

## 1 Introduction

The possible existence of neutrino oscillations is one of the most important issues in particle astrophysics as well as elementary particle physics at the present time. Among the positive and negative results reported for neutrino oscillation, experimental results for atmospheric neutrino by Super Kamiokande (hereafter, we abbreviate simply SK) has special position in the experiments concerned, because it is said that they have given the decisive and clear evidence for the existence of neutrino oscillation. The reasons as follows:

(1) They carried out the calibration experiments for the discrimination between muon and electron by electron accelerator beam whose energies are well known and established the clear discrimination between muon and electron for SK energy region concerned [1].

(2) Based on the well established discrimination procedure between muon and electron, they have analyzed *Fully Contained Events* and *Partially Contained Events*, whose energies covered from several hundreds MeV to several

GeV. As the results of them, they have found significantly different zenith angle distribution between for muon and electron, namely, muon deficit and attributed such discrepancy to the neutrino oscillation between muon and tau. As the most new one, they give  $\sin^2 2\theta > 0.92$  and  $1.5 \times 10^{-3} \text{eV}^2 < \Delta m^2 < 3.4 \times 10^{-3} \text{eV}^2$  at 90% confidence level [2].

(3) Also, they have analyzed *Upward Through Going Particle Events* and *Stopping Particle Events*. Most physical events under such category could be regarded as exclusively the muon (neutrino) induced events, not electron (neutrino) induced events, because the effective volume for muon is much larger than that for electron due to longer range of muon irrespective the discrimination procedure between muon and electron which is indispensable for the analysis for *Fully Contained Events* and *Partially Contained Events*. Also, in this case, they have given the same parameters for neutrino oscillation which are obtained in the analysis of *Fully Contained Events* and *Partially Contained Events* [2].

Through three different kinds of the experiment performed by SK, all of which are constructed upon the well established procedure, it is said that SK has given clear

and definite evidence for existence for the neutrino oscillation.

The analysis of *Fully Contained Events* and *Partially Contained Events* is closely and inevitably related to the discrimination procedure between electron and muon. Because the frequency of muon events with some energy occurred inside the detector is nearly the same as that of electron events unless oscillation exists and, therefore, the precise discrimination procedure between electron and muon is absolutely necessary.

Considering the great impact of SK experiment over other experiments concerned and theoretical physics, we feel we should examine the validities of the experimental results performed by SK, because nobody has examined them in the most comprehensive way, solely due to character of huge experiment, although the partial aspect of SK had been examined in fragmental way [3].

However, Mitsui et al have examined the validity of the discrimination procedure by SK and have pointed out the necessity of fluctuation effect into the discrimination procedure between muon and electron by SK [4].

We have examined validities of all the SK experiment, adopting quite different approach from the SK procedure.

In order to interpret the detected events (i.e. to define the CAUSES for the CONSEQUENCES) one should first go from CAUSES to CONSEQUENCES, i.e. solve a DIRECT problem, and then back from CONSEQUENCES to CAUSES, thus solving an INVERSE problem. SK solve the DIRECT problem in a rather simplified way and mostly concentrate on the INVERSE problem. We go both ways with reasonable care.

For the purpose, we have performed computer numerical experiments for examination of the validities of SK experimental results, constructing the virtual SK detector in the computer, the scale of which is same as the real SK detector.

Concretely speaking, firstly, we have constructed the virtual small scale of SK detector, the scale of which is the same as the real SK detector (small scale) for being exposed to the accelerator beam, in the computer, for testing the validity of the discrimination between muon and electrons adopted by SK. <sup>1</sup> SK utilize their results by simple extrapolation.

Based on the information obtained from the virtual small scale of the detector, we have constructed the full size scale of the virtual SK detector, the size of which is the same as that of the real SK detector in the computer and have really checked whether the clear discrimination which SK assert is possible or not. In this case, we take account of the difference in the size between the pilot detector for the accelerator beam and the real (full size) detector. The methodology adopted by us is described in the present paper. In a pair of subsequent papers, we really compare our results under our methodology (present paper) with SK results. Further, the analysis of both *Fully Contained*

*Events* and *Partially Contained Events* and the analysis of both *Upward Through Going Muon Events* and *Stopping Muon Events* in the numerical computer experiments will appear in the subsequent papers.

An analysis of *Fully Contained Events* and *Partially Contained Events* is given in a subsequent paper. An analysis of *Upward Through Going Muon Events* and *Stopping Muon Event* will be presented elsewhere.

From the methodological point of view for the analysis of the SK data, there should be two essential differences between the SK procedure and our procedure in the general analysis of physical events.

The first: as we already mentioned above, SK oversimplifies the solution of the DIRECT problem, namely, their mean models of both electron and muon events are too far from reality to be used in the INVERSE problem solution, while our mean models are reasonably accurate. The second: SK neglects fluctuation effects in physical processes in which the Cherenkov light is produced, while we consider them as correctly as possible, which we discuss in the section 2 and the subsequent sections.

In this paper, we limit our discussion to the discrimination procedure between muon and electron in the SK experiment (the item(1) in the Introduction)

The contents of the paper are organized as follows: In the section 2, we examine the SK standard discrimination procedure in detail. We examine the point-like approximation in the electron shower due to electron neutrino adopted by SK and conclude that such approximation leads to serious error in the energy determination of the electron neutrino. Next, we examine the probability functions for the pattern part and the angular part in both muon and electron and conclude that such separation of the pattern part from the angular part is not adequate and further, there are, a priori, no reasons why the probability functions for muon obey the same type of that for the electron, even if such separation is valid.

There are many factors which produce various errors in the SK discrimination procedure. The simple algebraic sum of such errors not always denote right resultant errors. In our discrimination procedure, we examine the resultant errors from the SK standard discrimination procedure, for example, the error in the vertex points of the neutrino interactions and their directions and more precise values.

In the section 3, we develop more suitable discrimination procedure instead of the SK standard procedure and, for the purpose, construct the mean angular distribution functions for Cherenkov light due to muon and electron and the corresponding relative fluctuation functions which make it possible to estimate the degree of the separation between muon and electron, errors of the vertex points for muon-like event and electron like events, the error of the directions due to these events. In a subsequent paper, we develop the general procedure for estimating the concrete errors for the neutrino events concerned and give finally various errors for the neutrino events quantitatively by comparing our results with SK results.

<sup>1</sup> The detailed study for the discrimination between electron and muon by using accelerator was carried out in Kasuga [5],[6] and Sakai[7].

## 2 Examination of the SK discrimination procedure between muon and electron

The approach for the discrimination between muon and electron adopted by SK is as follows.

(1) SK calculate Cherenkov images for electron and muon events by statistical and deterministic numerical methods but while constructing the pattern recognition procedure all fluctuation data and some important features of the mean models are completely ignored which are discussed below. Such manipulation leads to serious error in both pattern recognition between electron and muon and their energy estimation.

(2) Based on the Cherenkov light of the particle concerned mentioned above, SK constructed the probability function, ESTIMATOR for the particle identification, which is composed of pattern part and the angular part in the separated form.

The probability function for pattern,  $P_{pattern}(e(\mu))$ , which will appear in the section 2.2, denotes the pattern of the events concerned, namely, spatial and angular image of the events concerned. However, the variety of the images of the events concerned in SK discrimination procedure exclusively come from the fluctuations in the photoelectrons in the PMT, but not from the physical processes of the events concerned which produce the Cherenkov light, while in our procedure the image of the events concerned are essentially governed by the physical processes concerned which are completely neglected in the SK procedure.

The probability function for the angular part is introduced into the total probability (estimator for particle identification), being separated from that for pattern part. This is unnatural, however, because the pattern is of the concept on the space-angular structure. And it is natural that the concept of the angular should be included in the concept of the pattern. In our procedure, we construct the concept of the pattern as the angular-space image in which the spatial one is interrelated with the angular one (See, section 3.3).

Further, SK adopt the same type of the probability functions for muon and electron. However, there are no reasons why the probability function for muon obeys that for electron, because the generation mechanism of the total Cherenkov light is quite different in muon from in electron.

In present paper, we would emphasize the neglect of the fluctuation effects and the oversimplification in the problems adopted by SK lead to serious errors on the discrimination between muon and electron, which are shown in the present section and subsequent sections.

### 2.1 The Cherenkov light calculation for electron and muon.

#### 2.1.1 Examination on the Treatment of Cherenkov light for electron by SK

The SK analysis approximates the sources of the Cherenkov light due to electron showers as being point. In the calculation of the source for the Cherenkov light due to shower particles, the SK analyze electron events in average values, neglecting fluctuation and further assigns them to be point-like source. Such a treatment is not valid for the analysis of the real physical events concerned in the SK detector, because the sources for the Cherenkov light due to shower particles definitely have geometrical extents. The geometrical extent of electron cascade shower as a light source is not negligible compared with the scale of the SK detector.

Thus, the introduction of the point-like approximation into the construction of the ESTIMATOR for particle identification generally invites not negligible error into the analysis of experimental events. In what follows, we examine the limitations of the point-like approximation by SK. Here, we restrict our examination to the direct Cherenkov light, because the scattered Cherenkov light is not essential for the examination of the logical structure of the SK discrimination between electron and muon and we are exclusively interested in the logical structure of the SK procedure.

In order to construct the ESTIMATOR for electron identification, the SK calculate the mean number of photoelectrons which are produced by the Cherenkov light due to an electron-primary cascade shower (electron neutrino) using the Monte Carlo method. Thus, SK obtains,  $N_{i,exp}(direct)$ , the expected number of photoelectron from the direct Cherenkov light initiated by an electron in the  $i$  th PMT at a distance and an angle, in the following : [6], [7], [8]

$$\begin{aligned} N_{i,exp}(direct) &= \\ &= \alpha_e \cdot N_{MC}(\theta_i, p_e) \cdot \left(\frac{16.9}{l_i}\right)^\gamma \cdot \exp\left(-\frac{l_i}{L}\right) \cdot f(\Theta), \end{aligned} \quad (1)$$

where  $N_{MC}(\theta_i, p_e)$  denotes the mean number of the photoelectrons received in a circular area of 50 cm diameter located on a sphere of 16.9 meter in radius by the Full Monte Carlo simulation,  $\alpha_e$  is the normalization factor,  $l_i$  is the distance from the particle position to the  $i$  th PMT,  $\theta_i$  is the angle of the  $i$  th PMT from the particle direction, and  $f(\Theta)$  is the effective photo-sensitive area of the PMT. Here,  $L$  is the attenuation length of the Cherenkov light in the SK detector, which is taken 100 meter. The third term in the right-hand side of Eq.(1) shows the attenuation of light and its power index is estimated from Monte Carl simulation. The value of  $\gamma$  is 2.0 in Takita (p83, in [9]) and Kasuga(p32 in [5]) and Sakai(p41 in [7]), and 1.5 in Kasuga(p71 in [6]). A numerical value of 2.0 is used in older analysis while 1.6 is adopted in more recent work. The expression of Eq.(1) is an oversimplification on

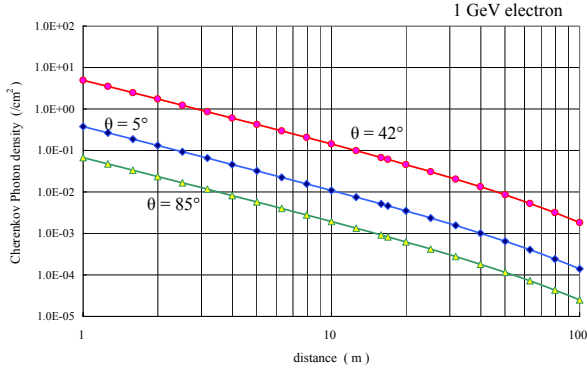


**Fig. 1.** The dependence of the Cherenkov photon density due to the electron shower on the distance for different angle from the direction of an incident 1 GeV electron with the point-like approximation, normalized with the values at 16.9m in Figure 2. The angles considered are 5, 42 and 85 degree. Sampling numbers of Monte Carlo simulations are 10000 per each angle. See the text for detail.

the estimation of photoelectrons by the Cherenkov light when we consider the real behaviour of the electron cascade shower. In order to clarify the oversimplification of the SK procedure, let us compare it with our procedure in the level of Cherenkov light, but not in the photoelectron level, because it is enough for the purpose concerned. Here, we could define the following expression which correspond to Eq.(1),

$$N_{exp,cher,app}(direct) = \alpha'_e \cdot N_{MC,cher}(\theta, p_e) \times \left(\frac{16.9}{l}\right)^\gamma \times \exp\left(-\frac{l}{L}\right), \quad (2)$$

where  $N_{MC,cher}(\theta, p_e)$  is the mean Cherenkov photon density which correspond to  $N_{MC}(\theta_i, p_e)$  in Eq.(1),  $\alpha'_e$  is another normalization factor and other parameters are same as in Eq.(1). Namely, Eq.(2) gives the Cherenkov photon density for the electron cascade shower under the point-like approximation which is utilized by SK. The dependence of the Cherenkov photon density  $N_{exp,cher,app}(direct)$  on the distance  $l$  is essentially determined by  $(16.9/l)^\gamma$  rather than  $\exp(-l/L)$ , because the attenuation of the Cherenkov light is small (100 meter of attenuation length in SK). Thus, the Cherenkov light depends strongly on the inverse power of the distance in the SK procedure.

In Figure 1, the dependence of the Cherenkov photon density due to the electron cascade shower on the distance ( $l$ ) are given for different angle from the direction of an incident 1 GeV electron with the point-like approximation using Eq.(2). The energy value of 1 GeV is a typical energy in the SK detector.

In order to examine the validity of the point-like approximation by SK, we have carried out the calculation of  $N_{exp,cher,FMC}(direct)$ , the Cherenkov photon density without the point-like approximation in Eq.(3) for the

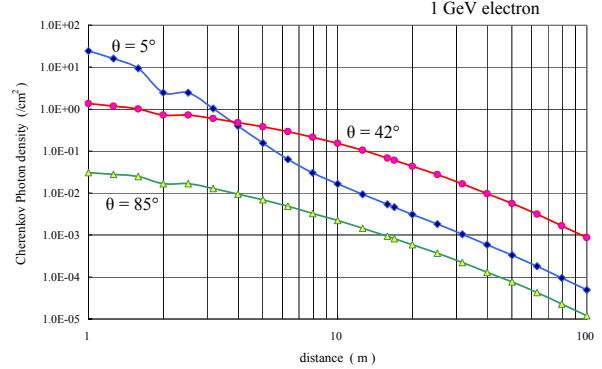


**Fig. 2.** The dependence of the Cherenkov photon density due to the electron shower on the depth for different angle from the direction of an incident 1 GeV electron without the point-like approximation. The angles considered are 5, 42 and 85 degree. Sampling numbers of Monte Carlo simulations are 10000 per each angle. See the text for detail.

comparison with Eq.(2). Instead of the point-like approximation, we simulate the electron cascade shower exactly in the stochastic manner, which we call [without point-like approximation]. Then, the Cherenkov photon density generated by the shower electron is calculated by help of GEANT3.21.

Namely, Eq.(3) denote the straightforward expression for the Cherenkov light density which is directly derived from the electron cascade shower without the approximation of  $(16.9/l)^\gamma$  and  $\exp(-l/L)$ . Thus, the definition of [without point-like approximation] denotes that we simulate electron cascade shower and accompanied Cherenkov light density in three-dimensional way at any distance and angle as exactly as possible. Namely, we calculate the whole structure of the Cherenkov photon density, taking into account the attenuation of light, as well as that of the electron cascade shower. Then, we obtain

$$N_{exp,cher,FMC}(direct) = N_{MC,cher,FMC}(\theta, p_e, l), \quad (3)$$

where  $N_{MC,cher,FMC}(\theta, p_e, l)$  denotes the Cherenkov photon density at the distance  $l$  without introducing the point-like approximation, which is obtained by the Monte Carlo method, taking into account the attenuation length of the Cherenkov light correctly.

In Figure 2, the dependence of the Cherenkov photon density on the distance without point-like approximation is given for the different angles from the direction of the incident electron using Eq.(3). In [without point-like approximation], the dependence on the distance and the attenuation are automatically included into functions themselves.

From the Figure 1, it is clear that the dependences of the Cherenkov photon density on the distance in the SK are same irrespective of the angles, which simply reflects the separation of the distance part from the angular part

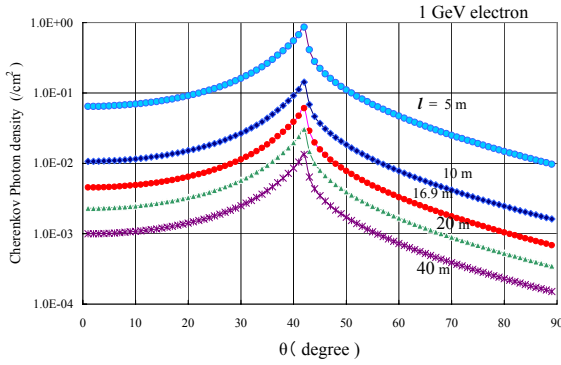


**Fig. 3.** Cherenkov photon density as a function of angle for different distances with the point-like approximation normalized with the values at 16.9 m in Figure 4 for 1 GeV primary electron.

in Eq.(2). Comparing the Figure 2 with Figure 1, it is easily understood that in the region beyond about 10 meter, the point like approximation is well approximation as far as the tendency in concerned, except the absolute values, while in the region inside about 10 meter, this approximation does not hold anymore, due to the actual longitudinal and lateral structure of the electron cascade showers. In particular, for direction within 5 degree, the effect of the lateral spread of the electron cascade shower as well as that of the definite longitudinal length becomes effective and the actual dependence on the distance is deviated largely from that in the point-like approximation.

In Figure 3 and Figure 4, we give the angular dependence of the Cherenkov photon density for different distances [with point like approximation](Eq.(2)) and [without point like approximation](Eq.(3)), respectively. In Figure 3, the shapes of their angular dependence is exactly same irrespective of their distance, because their angular part is separated from their distance part, as shown in Eq.(2). Such separation of the angular part from the distance part does not reflect real situation of the Cherenkov light density for electron, as shown in Figure 4.

In Figure 4, we give the corresponding ones to Figure 3 in the case of without point-like approximation. It should be noticed that for the region of smaller than 5 m the tendency of the angular dependence on angle is largely deviated from that for the region of larger distances. This reflects the fact that the Cherenkov photon density is largely influenced by the longitudinal and lateral structure of the real electron cascade shower. From figure 1 to 4 normalization are made at 16.9 meter.

In Table 1, we give the ratio of the Cherenkov photon density with the point like approximation to that without the point-like approximation for the exponent of 1.5(Kasuga,p74[6]). In Table 2, we give the same quantities for the exponent 2.0, the older value used in the SK analysis(Takita,p83[9], Sakai,p41[7]). The ratios are nor-

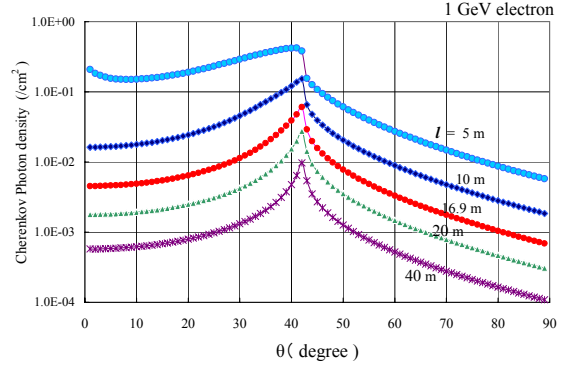


**Fig. 4.** Cherenkov photon density as a function of angle without the point-like approximation for 1 GeV primary electron. Other parameters are the same as in Figure 3.

**Table 1.** The ratio of the Cherenkov photon density from electron showers with the under point-like approximation (Eq.(2),  $\gamma = 1.5$ ) to corresponding ones without the point-like approximation (Eq.(3)). The primary energy of electron is 1 GeV.

angle (degree)	distasnce (m)				
	5.00	10.00	16.90	20.00	40.00
5	0.175	0.553	1.000	0.948	1.452
10	0.191	0.548	1.000	0.949	1.457
20	0.200	0.525	1.000	0.956	1.494
30	0.231	0.495	1.000	0.973	1.583
40	0.549	0.640	1.000	0.939	1.505
50	0.757	0.756	1.000	0.887	1.135
60	0.715	0.739	1.000	0.893	1.166
70	0.708	0.736	1.000	0.893	1.171
80	0.708	0.737	1.000	0.892	1.167
85	0.706	0.737	1.000	0.891	1.164

**Table 2.** The ratio of the Cherenkov photon density from electron showers with the point-like approximation (Eq.(2),  $\gamma = 2.0$ ) to corresponding ones without the point-like approximation (Eq.(3)). The primary enegy of electron is 1 GeV.

angle (degree)	distasnce (m)				
	5.00	10.00	16.90	20.00	40.00
5	0.322	0.719	1.000	0.872	0.944
10	0.352	0.712	1.000	0.872	0.947
20	0.368	0.682	1.000	0.879	0.971
30	0.425	0.643	1.000	0.894	1.029
40	1.009	0.832	1.000	0.863	0.978
50	1.393	0.983	1.000	0.815	0.738
60	1.314	0.960	1.000	0.821	0.758
70	1.301	0.956	1.000	0.821	0.761
80	1.301	0.958	1.000	0.820	0.758
85	1.299	0.958	1.000	0.819	0.757

malized to the values in Eq.(3) at the 16.9 meter in the both cases.

Comparing Table 1 and Table 2, it is clearly understood that the ratios depend strongly on the values of  $\gamma$ . If the point like approximation is valid, then, the ratios in Table 1 and Table 2 should remain around 1.0 with satisfactory allowance for every distance and every angle. However, it is clear from the tables such situation is never realized. SK guarantee the accuracy of the energy determination for the event is within  $\pm 2.6\%$  (Ishitsuka  $\pm 2\%$  (p29 in [10]), Kameda  $\pm 2.5\%$  (p62 in [11]), Okumura  $\pm 2.5\%$  (p45 in [12]), Messier  $\pm 2.5\%$  (p92 in [13]) and Kasuga  $\pm 2.6\%$  (p53 in [6])). This is quite far from the reality. In conclusion, Eq.(1), the expression for the photoelectron utilized by SK, does not consider the longitudinal and lateral structure of the electron cascade and, therefore, an oversimplification which could not estimate the photoelectrons by the Cherenkov light correctly.

### 2.1.2 Cherenkov light for muon

In contrast to the case of electron, SK calculates the Cherenkov light, taking into account the definite extent of muon range, namely, without point-like approximation. However, still, SK neglect the fluctuation effect. Here, let us examine the validity of the expression adopted by the standard SK analysis for a muon event, in which the expected number of photoelectrons in the  $i$  th PMT produced by a muon is expressed as Takita(p84 in [9]),

Sakai(p41 in [7]), Kasuga(p74 in [6]), Kibayashi(p71 in [8]),

$$N_{i,exp}(direct) = \left\{ \alpha_\mu \times \frac{1}{l_i(\sin\theta_i + l_i \times (\frac{d\theta}{dx}))} \times \sin^2\theta_i + N_{i,knock}(\theta_i) \right\} \times \exp\left(-\frac{l_i}{L}\right) \times f(\Theta), \quad (4)$$

where  $\alpha_\mu$  is the normalization factor. The second term in the right-hand side originates from the ionization energy loss  $dE/dx$  in water. Taking into account the change in the photon density which is caused by the change in, corresponding to the energy loss,  $dx\sin\theta + l d\theta$ , expresses the intensity variation of the Cherenkov photons.

$N_{i,knock}(\theta_i)$  shows the number of expected photons from knock-on electrons as a function of, which is estimated by a Monte Carlo simulation. It is easily understood from Eq.(4) that the logic for producing photoelectron in the muon is definitely deterministic. In other words, the SK analysis neglects fluctuation effects on the generation of the Cherenkov light from muon completely. However, the muon losses its energy and changes the direction in stochastic way, namely, knock-on, the decay-product electron and multiple scattering. Therefore, we could not neglect fluctuations for the muon event. As one example of muon behavior, we show the range fluctuations for muon in Figure 5. The neglect of fluctuations for muon causes uncertainty in the estimation of the muon energy.

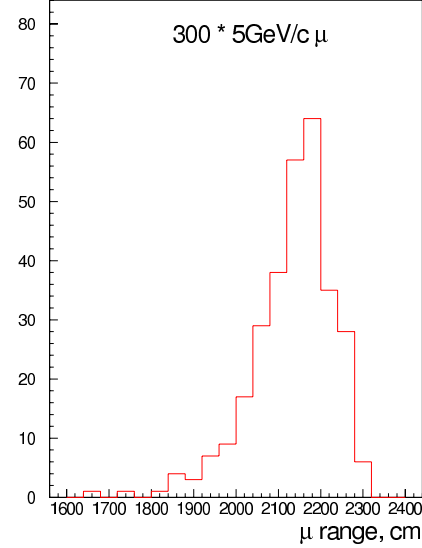


**Fig. 5.** Range fluctuation of 5 GeV muons. The number of simulation is 300.

## 2.2 Pattern recognition procedure adopted by SK

In previous subsection, we examine accuracies on the Cherenkov light quantities for electron and muon, which is related to the estimation of the energies of the particles concerned directly for the Fully Contained Events. In the present section, we should like to say these quantities are of major importance for the type definition and geometry recognition, both in SK and our case. Here, we examine pattern recognition procedure for the particle concernrd.

### 2.2.1 Principle of the ESTIMATOR of particle identification adpted by SK

SK defines the probability,  $Prob_i(N_{exp}, N_{obs})$ , suitable for the particle identification. It is the probability to observe the number of photoelectron,  $N_{obs}$ , for an expected mean number of photoelectron,  $N_{exp}$ . The  $N_{obs}$  actually deviates from the ideal Poisson distribution due to fluctuations in amplification processes of the PMTs. The probability function is simply given by:

$$Prob = \frac{1}{\sqrt{2\pi\sigma}} \exp\left(-\frac{(N_{obs} - N_{exp})^2}{2\sigma^2}\right), \quad (5)$$

where  $Prob_i$  is the probability function for the  $i$  th PMT. Thus, SK define the likelihood functions for e-like event and mu-like event is the following:

$$L_e = \prod_{\theta_i < (1.5 \times \theta_c)} Prob_i(e), \quad (6)$$

$$L_\mu = \prod_{\theta_i < (1.5 \times \theta_c)} Prob_i(\mu),$$

where  $Prob_i(e)$  is calculated assuming the event is due to electron. And  $Prob_i(\mu)$  due to muon. In order to combine the information of the Cherenkov opening angle with

the information of the ring pattern,  $L_e$  and  $L_\mu$  are transformed into  $\chi^2$  distribution so that SK obtain the following functions for spatial part and angular part.<sup>2</sup>

$$P_{pattern}(e) = \exp \left\{ -\frac{1}{2} \left( \frac{\chi^2(e) - \min[\chi^2(e), \chi^2(\mu)]}{\sigma_{\chi^2}} \right)^2 \right\}.$$

$$P_{pattern}(\mu) = \exp \left\{ -\frac{1}{2} \left( \frac{\chi^2(\mu) - \min[\chi^2(e), \chi^2(\mu)]}{\sigma_{\chi^2}} \right)^2 \right\}. \quad (7)$$

$$P_{angle}(e) = constant \times \exp \left\{ -\frac{1}{2} \left( \frac{\theta_{exp}(e) - \theta_{obs}}{\Delta\theta} \right)^2 \right\}$$

$$P_{angle}(\mu) = constant \times \exp \left\{ -\frac{1}{2} \left( \frac{\theta_{exp}(\mu) - \theta_{obs}}{\Delta\theta} \right)^2 \right\} \quad (8)$$

Combining (6) with (7), SK obtains probability functions for electron and muon finally in the following:

$$P(e) = P_{pattern}(e) \times P_{angle}(e), \quad (9)$$

$$P(\mu) = P_{pattern}(\mu) \times P_{angle}(\mu).$$

A ring is more mu-like than e-like, if  $P(\mu) > P(e)$  and vice versa.

### 2.2.2 Examination of the components of the ESTIMATOR adopted by SK

Let us examine the validity of Eq.(5) in the SK procedure. [1] They neglect fluctuation effects in physical processes for electron and muon. SK introduce Eq.(5) for the detection of the particle concerned. However, they consider only fluctuation effect coming from the amplification processes in the PMT, namely, electro-mechanical effect of the hardware detector, and never any fluctuation effect coming from the physical process for electron and muon, namely, fluctuation from shower particles for electron (neutrino) and range straggling of muon for muon (neutrino) which play essential role for formation of variety of the pattern onto the detector for electron and muon. Namely, SK describe the behavior of electron and muon in the mean values. Consequently, varieties of the Cherenkov light pattern due to electron and muon are produced only through "Poison distribution in the amplification process in the PMT, the position of the neutrino interaction and the direction of the incident neutrino. However, essential character of the varieties of the Cherenkov light due to

electron and muon are only produced through the fluctuation in the physical processes of the particle concerned. If we consider fluctuation effect correctly, Eq.(1) defined by SK should be replaced by

$$P_e(N : E_0) = P_e(N_{e,obs}, N_{e,exp}(E_0)) \times P_e(N, N_{e,obs}), \quad (10)$$

where  $P_e(N : E_0)$  denotes the probability for an electron with energy  $E_0$  to produce a cascade shower in which  $N$  photoelectron are produced by the Cherenkov light due to shower particles.  $P_e(N_{e,obs}, N_{e,exp}(E_0))$  is the probability for an electron with primary energy  $E_0$  and the mean number of the Cherenkov photon,  $N_{e,exp}(E_0)$ , to produce the observed number of the Cherenkov photons,  $N_{e,obs}$  and  $P_e(N, N_{e,obs})$  denotes the probability for  $N_{e,obs}$ , number of the Cherenkov photons to produce finally the number of the photo-electron  $N$ .  $P_e(N_{e,obs}, N_{e,exp}(E_0))$  shows the fluctuation effect in a electron cascade shower and  $P_e(N, N_{e,obs})$  correspond to Eq.(5) in SK procedure. For muons, the expression which correspond to Eq.(8) is given as follows:

$$P_\mu(N : E_0) = P_\mu(N_{\mu+e,obs}, N_{\mu+e,exp}(E_0)) \times P_\mu(N, N_{\mu+e,obs}) \quad (11)$$

where  $P_\mu(N : E_0)$  is the probability for a muon of primary energy  $E_0$  to produce the number of the photo-electron  $N$  by the Cherenkov light due to the muon and its accompanying electron (knock on electron and others).  $P_\mu(N_{\mu+e,obs}, N_{\mu+e,exp}(E_0))$  shows the fluctuation effect in the physical processes of muon, namely, the range straggling of muon. Corresponding to Eq.(5),  $P_e(N, N_{e,obs})$  and  $P_\mu(N, N_{\mu+e,obs})$  may be approximated by Gaussian distribution with different  $N$ . However,  $P_e(N_{e,obs}, N_{e,exp}(E_0))$  should be different from  $P_\mu(N_{\mu+e,obs}, N_{\mu+e,exp}(E_0))$ , because the physical process for producing the Cherenkov light for electron is clearly different from that for muon. Consequently, there are no reasons, a priori, why  $P_e(N_{e,obs}, N_{e,exp}(E_0))$  and  $P_\mu(N_{\mu+e,obs}, N_{\mu+e,exp}(E_0))$  should obey the same Gaussian distribution. In conclusion, Eq.(9) lacks in theoretical background as the probability function in the practical application to the analysis of experimental data.

### 2.2.3 Resultant errors introduced by SK discrimination procedure

In previous subsection, we examine errors introduced into the Cherenkov light quantities for electron and muon. The final purpose of the construction of the ESTIMATOR adopted by SK is [a] the discrimination between electron and muon, [b] decision of the vertex position in the neutrino event and decision of the direction of the individual neutrino event and [c] the decision of the momentum of the particle concerned. Therefore, one may be very interested in the resultant errors which SK procedure invite

<sup>2</sup> In our opinion, a priori, there are no reasons why does the probability function for muon obey the same type of the probability function for electron.

due to inadequency of the ESTIMATOR, the neglect of the fluctuation effect and assumption of the point-like approximation.

The answer is as follows: we could not estimate individual error in the SK procedure, for example, the error due to the oversimplification in the treatment of the electron cascade shower. The individual error is intermingled with each other so that we get the resultant errors which are never the simple sum of the individual error. Namely, we could get the resultant errors only, for example, the error of the energy measurement in the neutrino events, the errors on the vertex in the neutrino event, the error on the direction of the neutrino even and so on.

In the next section, we develop our rigorous procedure which does not include inconsistency of the logic.

### 3 Principle of our discrimination procedure between electron and muon: Application of pattern recognition theory to e-mu discrimination.

#### 3.1 Overcome to the defect of the SK procedure

In the previous section, we clarify that the estimation of the Cherenkov light quantities due to the electron event and the muon event as well as the discrimination of their pattern are not reliable. Because, both electron events and muon events are recognized without taking their fluctuation effect which may kill the real variety of their pattern. In the electron events, the point-like approximation may lead serious misestimation of their as shown in Table 1 and Table 2. In order to overcome the defects inherent in the SK discrimination procedure, we develop our discrimination procedure as exactly as possible, taking the stochastic characters in the physical processes concerned carefully into account.

Here, we restrict the development of our theory at the level of the Cherenkov light, but not at the photoelectron level which are directly related to the actual experimental result as in the SK procedure. The reasons are as follows: The most important of our present paper is to clarify the essential defect adopted by SK and propose the direction of the possible alternative procedure by which SK procedure could be replaced.

In this case, it is enough for us to examine physical quantities in the level of the Cherenkov light leaving out the consideration of photon conversion into photoelectron. Such simplification reduces the overall uncertainties of parameter estimates and, thus, our results give the lower limits for the errors in the analysis of the neutrino events concerned. To illustrate the scale of uncertainty added by the light-to-electron conversion, in Figure 6 we give the probability distributions of the number of the Cherenkov photon for given number of photoelectron. Of course, while applying our methods to the analysis of the real experiment one should take photoelectron fluctuations into account.

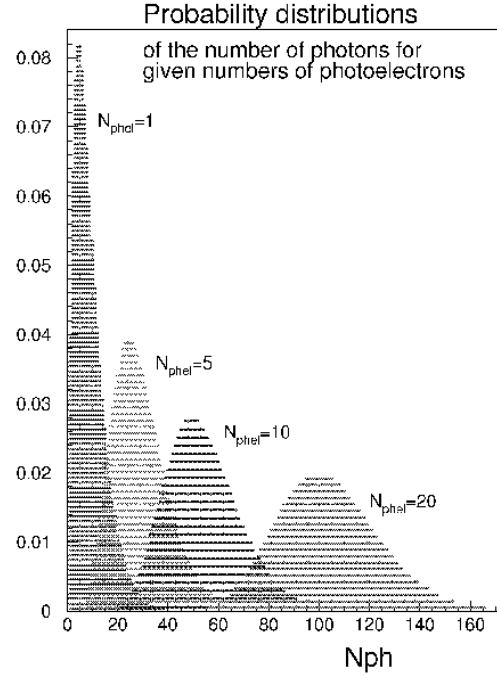


**Fig. 6.** fig:6 Probability distributions of the number of the Cherenkov photons for given numbers of photoelectron. The number of simulation is 100.

#### 3.2 Construction of a suitable procedure for the discrimination of muons from electrons

The examination described in the previous section leads us to conclude that the probability functions and the approximations used in the standard SK analysis are not reliable for the discrimination of muons from electrons. Therefore, a more reliable procedure, constructed on a solid theoretical basement, is required. Here, we will outline a more reliable and suitable algorithm for discrimination of muons from the electrons. First, we simulate the physical processes for the Cherenkov light as exactly as possible using GEANT 3.21, and construct new mean angular structure functions for the Cherenkov light for pattern recognition of the Cherenkov light due to both the muon and electron. Second, we derive their relative fluctuation functions for the Cherenkov light distribution which are critical for constructing an estimator for particle identification.

In our mean angular structure functions, we calculate the Cherenkov light due to both muon and electrons along the direction of the primary muon and electrons. Then, followings are considered.



(1) As for the mean longitudinal size of  $\mu$ -track/electron shower, we adopt the total longitudinal length ( $T_e$  defined lately) in which 99.5 percent of the total Cherenkov light are considered.

(2) The total longitudinal length along which the particles concerned emit the Cherenkov light is emitted is divided into a number of equal segments. The number of the division is dependent on the particle type, primary energy and the required accuracy of the image presentation.

(3) We calculate the mean angular distribution,  $F_i^{e,\mu}(\theta)$ , and its relative fluctuation  $\delta_i^{e,\mu}(\theta)$  for each segment  $i$ , and construct the mean angular distribution functions,  $F^{e,\mu}(\theta, t)$  and their relative fluctuations,  $\delta^{e,\mu}(\theta, t)$ , as function of radiation angle,  $\theta$ , and water layer thickness,  $t$ . The item(3) will be discussed in a subsequent paper

We neglect the lateral distributions of particles in both  $e$  and  $\mu$  events, i.e., we assume that all Cherenkov light is emitted at the event axis. This makes our approach invalid for events close and approximately parallel to the walls of the detector, but it is adequate for the particle discrimination quality estimates. The much simpler approach adopted in the standard SK analysis would result in larger errors in type and geometry reconstruction procedures, particularly in case of peripheral events when the longitudinal development of  $e$ -shower/ $\mu$ -track Cherenkov light angular distribution is most prominent.

Note that angular distribution functions for the Cherenkov light are universal functions for a given particle type and energy and can be used for calculating mean pattern images and their deviations for any required event geometry in any water tank.

Further, it should be noticed that we need not introduce  $P_{pattern}(e(\mu))$  and  $P_{angle}(e(\mu))$  in the procedure for the discrimination as in Eqs.(7) and (8) in the final probability function, and directly get the final probability function.

### 3.3 The construction of the mean angular distribution functions of Cherenkov light for muons and electrons

From the view point of pattern recognition, we need more accurate angular distribution functions for the total Cherenkov light due to both muons and electrons, rigorously taking into account fluctuations inherent in both types of event, to confirm the discrimination between muons and electrons. For this purpose, we construct angular structure functions for the Cherenkov light in the following way.

#### 3.3.1 The construction of the mean angular distribution function due to a primary electron and its relative fluctuation function.

An electron due to electron neutrino interaction produces an electron shower in which shower electrons are distributed over some range in space, each of which produces Cherenkov light. It is not suitable for such a range to be approximated by the point-like as assumed in SK, on which we have already clarified. Instead of the SK point-like approximation, we introduce a ‘moving-point’ approximation in the

following to construct the angular distribution function for the total Cherenkov light. Here, we construct the mean angular distribution function for the Cherenkov light for electron.

In a large water tank detector which is large enough for the dimensions of the electron showers concerned, we calculate the development of total Cherenkov light due to the electron shower.

We exactly simulate individual angular distributions for the Cherenkov light using a combination of GEANT 3.21 with the calculation tools developed by us. To construct the mean angular distribution function for the Cherenkov light and its relative fluctuation function accurately, we need to simulate a large number of showers, 10000 to 20000. Let  $T_e$  be the total length of an electron shower initiated by a primary electron. We divide  $T_e$  in segments, the length of which depends on the primary energy of the charged particle concerned and which is taken as 40 cm in present calculation.

Shower particles are produced according to the exact simulation procedure of the electron cascade shower, but in our models of the Cherenkov light, both the mean angular distribution function and corresponding angular distribution relative fluctuations function are attributed to a certain segment. When calculating the pattern images with the help of the models, all Cherenkov photons generating within the segment are thought to start from the middle of the segment. This approximation is called the ‘‘moving-point’’ (or ‘‘multi-point’’) approximation, in contrast to the single point approximation adopted in the standard SK analysis.

We simulate the cascade shower initiated by the primary electron and calculate the Cherenkov light from shower particles in each segment and obtain the angular distribution function for the Cherenkov light by distributing all the Cherenkov photons emitted from segment  $k$  over the bins of a histogram  $N_e(\theta, E_0, k)$  in  $\theta$  to estimate:

#### The Mean angular distribution function

$$F_e(\theta_i, E_0, k) = \frac{\langle N_e(\theta_i, E_0, k) \rangle}{\Delta\Omega_i}, \quad (12)$$

where  $\langle \dots \rangle$  denotes the average over a large event sample,  $\theta_i$  is the center of mass of the  $i$ -th histogram bin, and  $\Delta\Omega_i$  is the solid angle of the  $i$ -th bin.

#### The Relative fluctuation function for the angular distribution

$$\delta_e(\theta_i, E_0, k) = \frac{\sqrt{\langle N_e^2(\theta_i, E_0, k) \rangle - \langle N_e(\theta_i, E_0, k) \rangle^2}}{\langle N_e(\theta_i, E_0, k) \rangle}. \quad (13)$$

Then we fit the mean angular distribution (12) for each segment separately by a function:

$$F_e(\theta, E_0, k) = 10^{\{[A + B3/(1+B \cdot |\theta - C|^{(B4+B1 \cdot |\theta - C|)})]/[1 + B2 \cdot \theta]\}}, \quad (14)$$

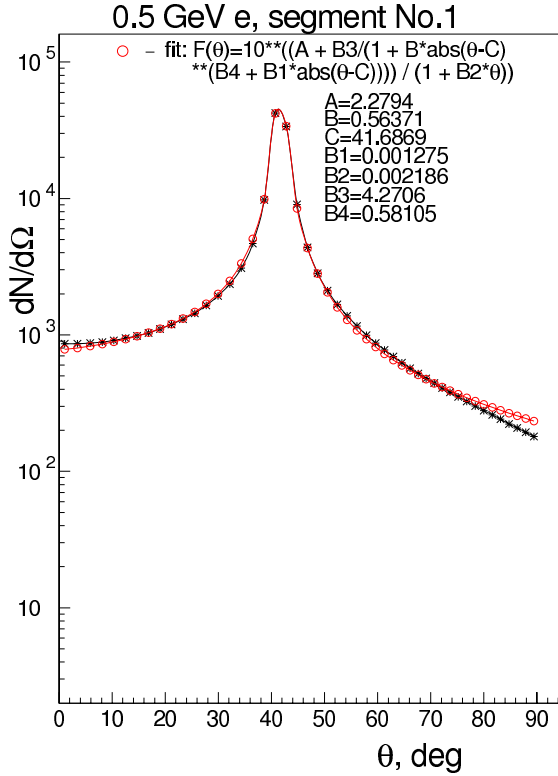


**Fig. 7.** fig:7a The angular structure function for 500 MeV electrons from segment No.1. See the text for details.

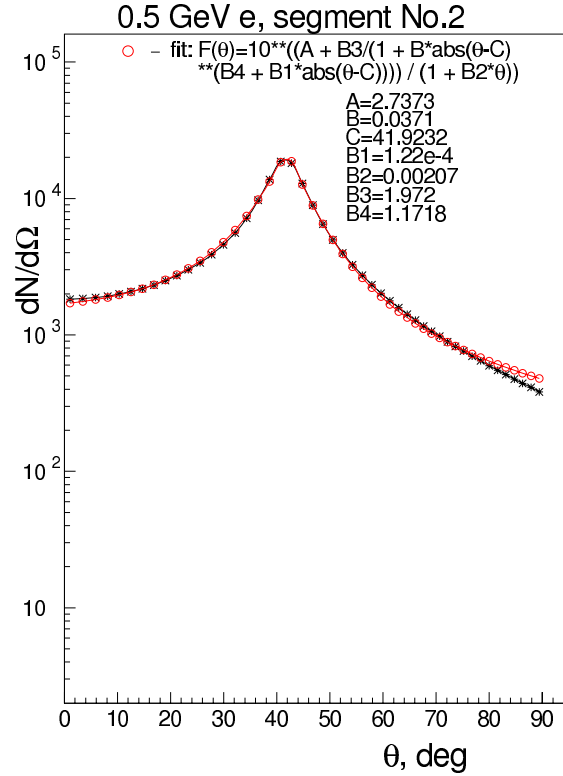


**Fig. 8.** fig:7b The angular structure function for 500 MeV electrons from segment No.2. See the text for details.

where the numerical values of A, B, C, B1, B2, B3 and B4 depend on the primary energy of the electron and the corresponding segment.

In Figures 7 to 11, we give the mean angular distribution function for the total Cherenkov light from each segment for a 500 MeV electron. We give the mean angular distribution function for the total Cherenkov light emitted in segments No.1 (the interval from 0 to 40 cm from the starting point of cascade shower), No.2 (from 40 cm to 80 cm from the starting point), No.3 (80 cm to 120 cm), No.4 (120 cm to 160 cm), and No.5 (160 cm to 200 cm), in Figures 7, 8, 9, 10 and 11, respectively.

The electron shower produced by a 500 MeV electron is rather small and the essential character of the cascade shower is determined in segments 1 to 5. In Figure 7 (segment No.1), which corresponds to the initial stage of shower development, shower particles are energetic and near the core of shower axis and so give rise to a strong peak around the Cherenkov angle due to energetic particles initiating the cascade shower. In Figure 8 (segment No.2), the cascade shower reaches shower maximum, where number of shower particles reaches a maximum, and the total Cherenkov light produced in this segment is roughly the same as that in segment No.1. However, the average energies of shower particles in this segment are smaller than those in segment No.1, and they are more scattered due to multiple scattering and so there is more deviation from the original Cherenkov angle.

The situation in segment No.3 (Figure 9) is roughly the same as that in segment No.2 (Fig.8). It should be

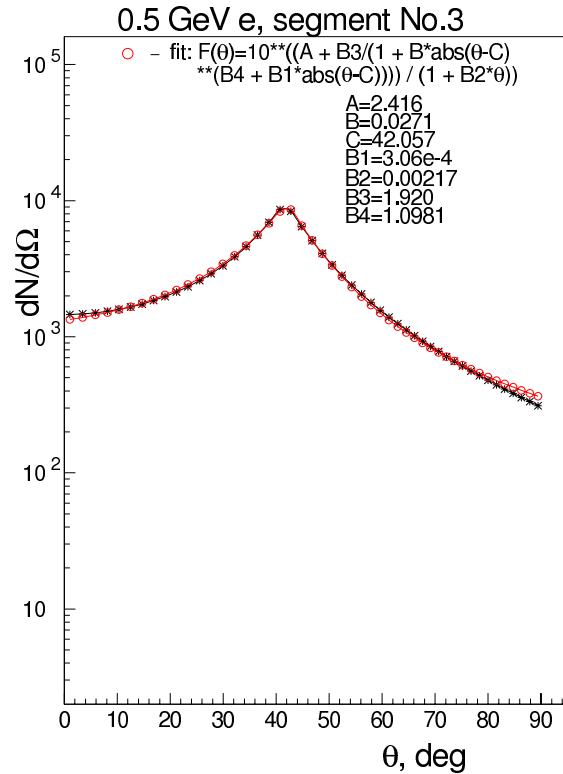


**Fig. 9.** fig:7c The angular structure function for 500 MeV electrons from segment No.3. See the text for details.

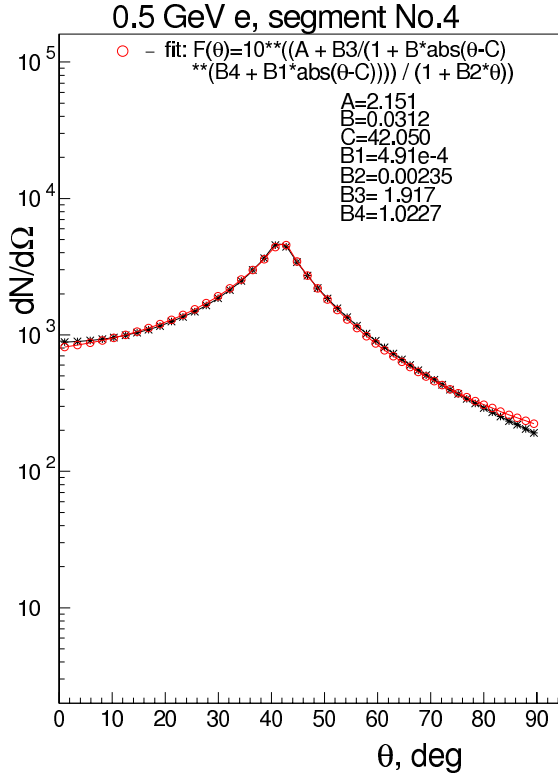


**Fig. 10.** fig:7d The angular structure function for 500 MeV electrons from segment No.4. See the text for details.

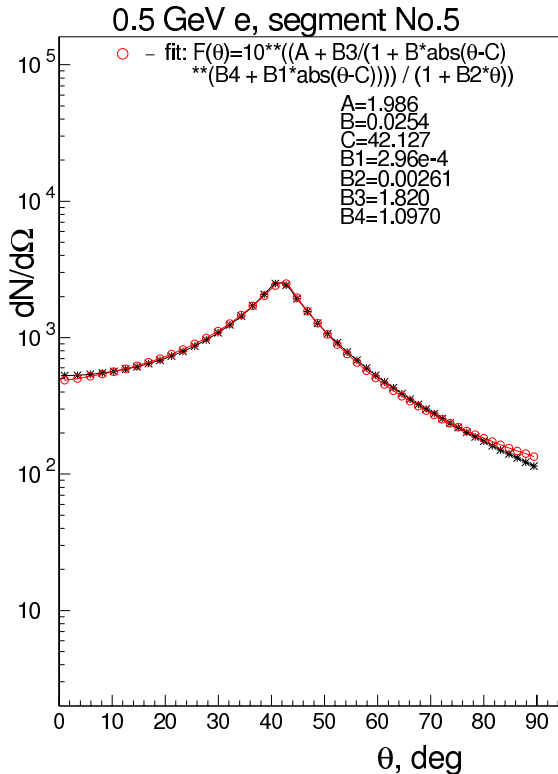


**Fig. 11.** fig:7e The angular structure function for 500 MeV electrons from segment No.5. See the text for details.

emphasized that the amounts of Cherenkov light emitted in segments No.2 and No.3 are greater than that in the segment No.1 (near the starting point of the cascade shower) at all angular regions except the original Cherenkov angle. Even in the segments No.4 (Figure 10) and No.5 (Figure 11), where electron shower is attenuated rapidly, the contributions of Cherenkov light from outside the original Cherenkov angle could not be neglected compared with that from the segment No.1, which is too near the starting point of the cascade shower. In conclusion, as the Cherenkov light produced in every segment contributes to the edge of the Cherenkov ring, we cannot say that the Cherenkov light at the edge of the Cherenkov ring comes exclusively from the starting point of the cascade shower (the vertex point of the electron neutrino reaction), which is the assumption adopted in the SK analysis (See Figure 2.9 in Sakai, [7]). Here, we have paid particular attention to a 500 MeV electron, however, such characteristics hold irrespective of the primary energy of the electron.

In order to calculate the relative fluctuation function for the angular distribution accurately, a large sample of simulated events is needed: we used 20000 events for  $E_0 \leq 500$  MeV and 10000 events for  $E_0 > 500$  MeV.

In Figures 12 to 16 we construct the relative fluctuation function for the Cherenkov light from a 500 MeV electron. The relative fluctuation functions are extremely important for the pattern recognition of electrons and muons. Therefore, we should determine them as accurate as possible, which was why we simulated such a large number of events.

In Figures 12, 13, 14, 15 and 16 we give the relative fluctuations for the Cherenkov light from segments 1, 2, 3, 4 and 5, respectively.

In Figure 12 (segment No.1), the shower particles are relatively energetic so that the relative fluctuation is a minimum near  $42^\circ$ , the original Cherenkov angle, as expected. In Figure 13 (segment No.2), the situation is the same as in Figure 12. It is interesting to note that the minimum disappears in the segment No.3 (Fig. 14) and a maximum appears at the original Cherenkov angle in segments No.4 (Fig. 15) and No.5 (Fig. 16). However, globally speaking, the angular dependence of the fluctuation is weak and it is relatively similar at all angles. Of course, this does not mean that shower particles are produced isotropically, losing the direction of the initiating particle.

The fluctuations in the electron events which are described above are quite different from those in muon events (see next subsection).

We need to take these relative fluctuations into account for more reliable discrimination between electrons and muons. This is the reason why we calculate the relative fluctuations after simulating each energy 10000 to 20000 times.

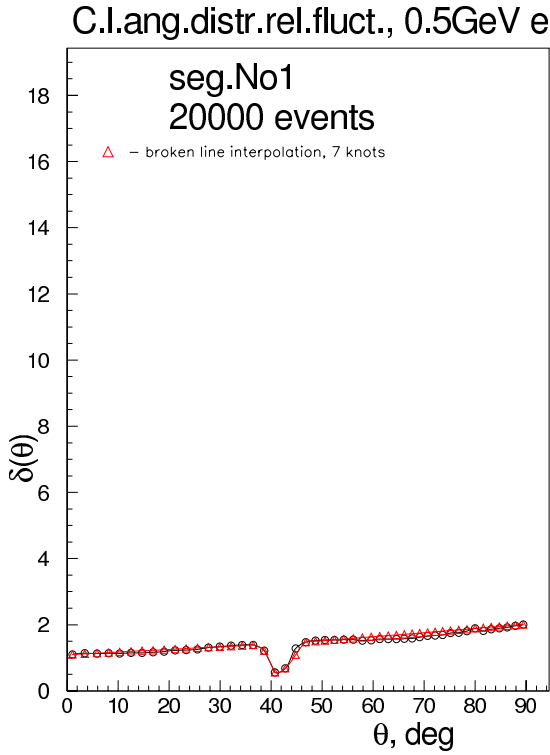


**Fig. 12.** fig:8a The relative fluctuations in the angular distribution of the Cherenkov light for 500 MeV electrons from segment No.1. See the text for details.

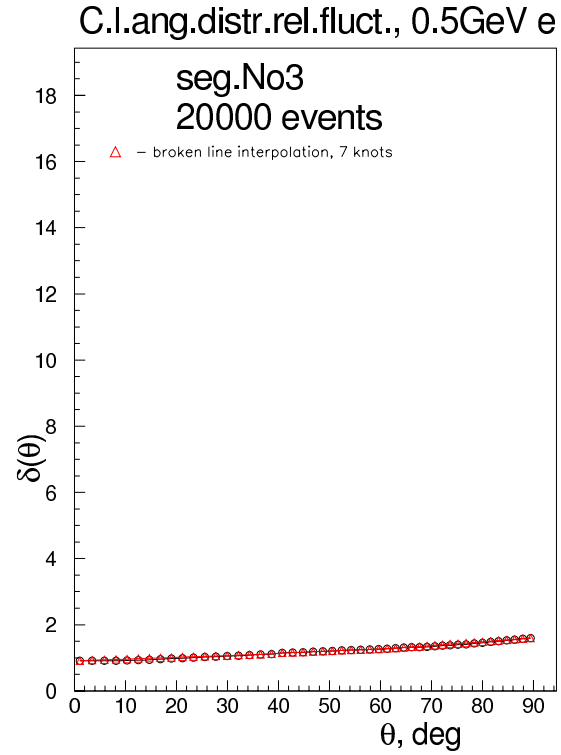


**Fig. 14.** fig:8c The relative fluctuations in the angular distribution of the Cherenkov light for 500 MeV electrons from segment No.3. See the text for details.

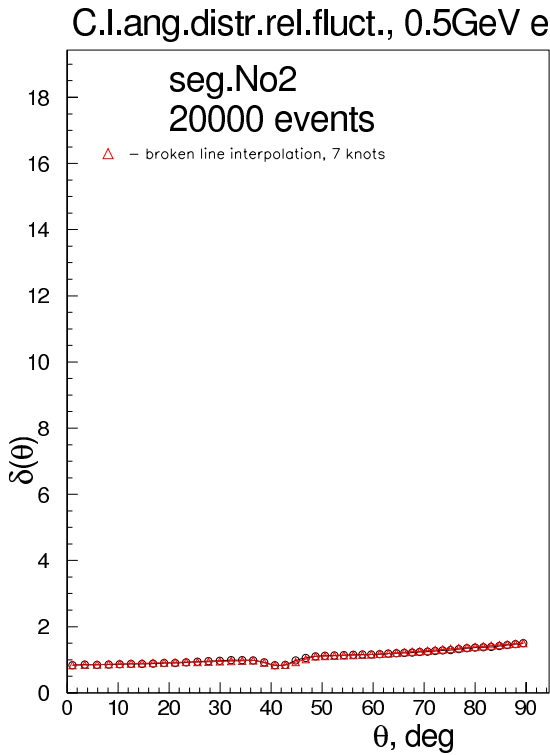


**Fig. 13.** fig:8b The relative fluctuations in the angular distribution of the Cherenkov light for 500 MeV electrons from segment No.2. See the text for details.

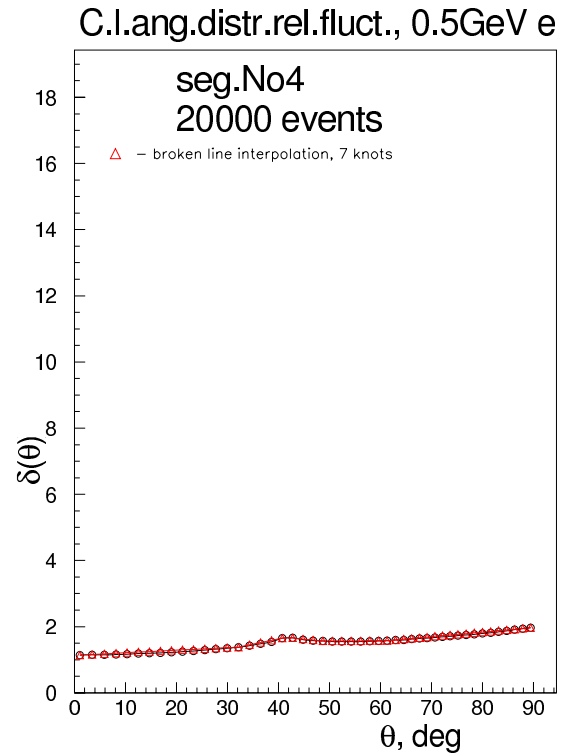


**Fig. 15.** fig:8d The relative fluctuations in the angular distribution of the Cherenkov light for 500 MeV electrons from segment No.4. See the text for details.

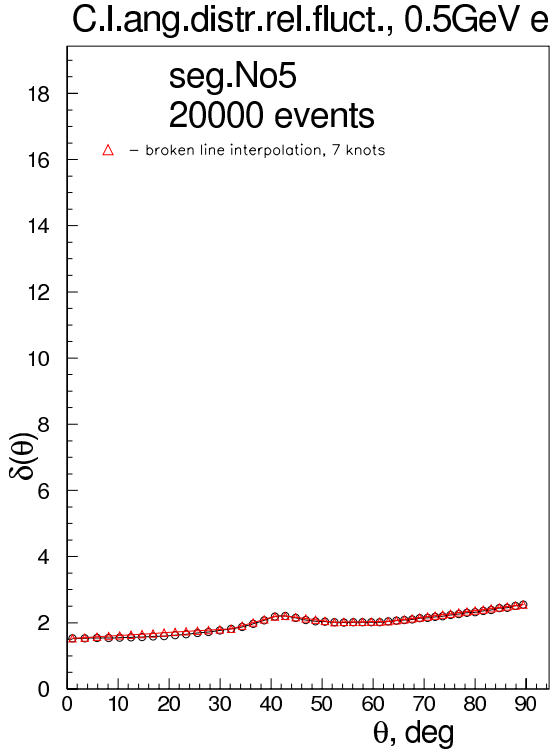


**Fig. 16.** fig:8e The relative fluctuations in the angular distribution of the Cherenkov light for 500 MeV electrons from segment No.5. See the text for details.

### 3.3.2 The construction of the mean angular distribution function due to a primary muon and its relative fluctuation function.

In the same way as in the preceding sub-section, we obtain the mean angular distribution function  $F_\mu(\theta, E_0, k)$  for the Cherenkov light emitted due to the primary muon and its relative fluctuation  $\delta_\mu(\theta, E_0, k)$ .

We then fit the mean angular distribution for each segment in turn by a function:

$$F_\mu(\theta, E_0, k) = 10^{\{A \exp[-B(\theta-C)^2]\}} + 10^{\{B1/(1+B2\theta^4)\}}, \quad (15)$$

where the numerical values of A, B, C, B1 and B2 are dependent on both  $E_0$ , the primary energy of muon, and  $k$ , the segment.

In Figures 17 to 21 we construct the mean angular distribution function for the total Cherenkov light from each segment for a 500 MeV muon. We give the mean angular distribution function for the total Cherenkov light due to segments No.1 (the interval from 0 to 40 cm from the starting point of cascade shower)(Fig.17), No.2 (40 cm to 80 cm) (Fig.18), No.3 (80 cm to 120cm)(Fig.19), No.4 (120 cm to 160 cm) (Fig.20) and No.5 (160 cm to 200 cm) (Fig.21) Comparing Figure 17 with Figure 7, one can easily understand that the peak around  $42^\circ$  in the case of the muon is very sharp compared with that in the case of the electron.

This means that the larger contribution of the Cherenkov light is due to muon itself and the contributions to either

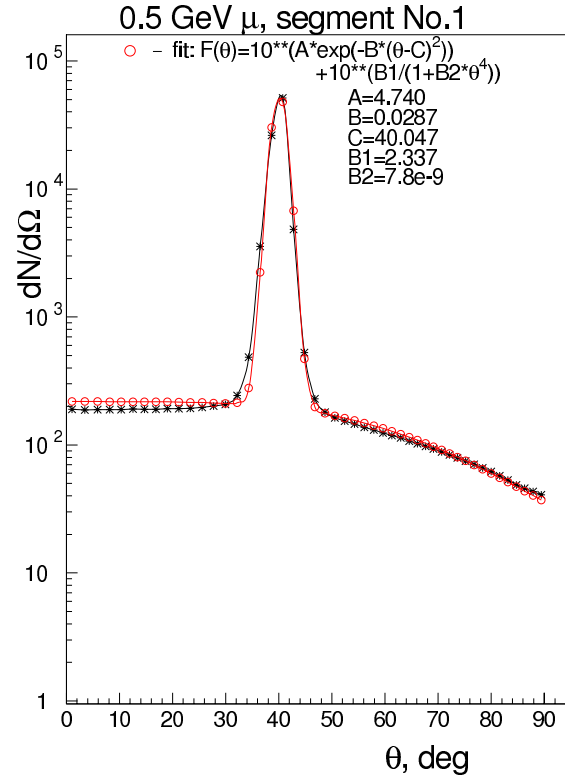


**Fig. 17.** fig:9a The angular structure function for 500 MeV muons from segment No.1. See the text for details.

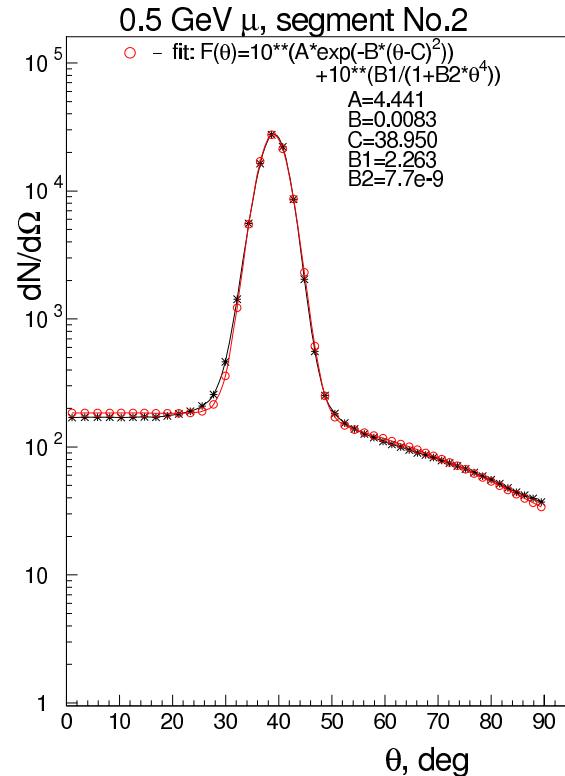


**Fig. 18.** fig:9b The angular structure function for 500 MeV muons from segment No.2. See the text for details.

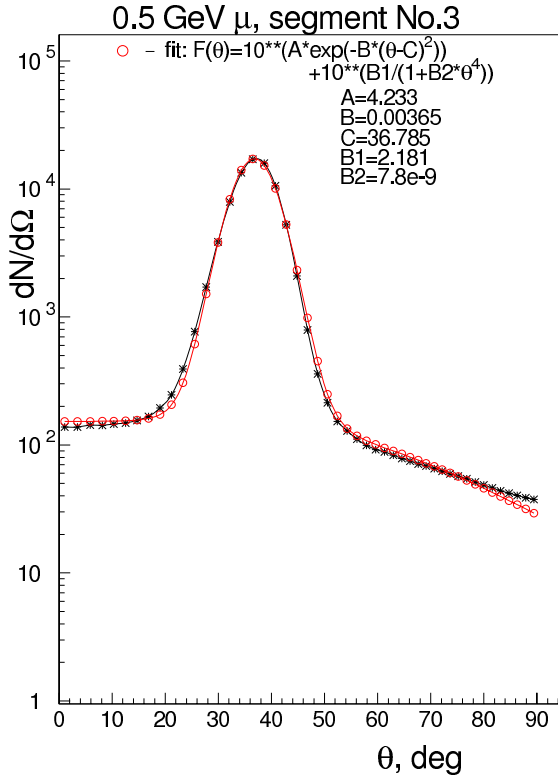


**Fig. 19.** fig:9c The angular structure function for 500 MeV muons from segment No.3. See the text for details.

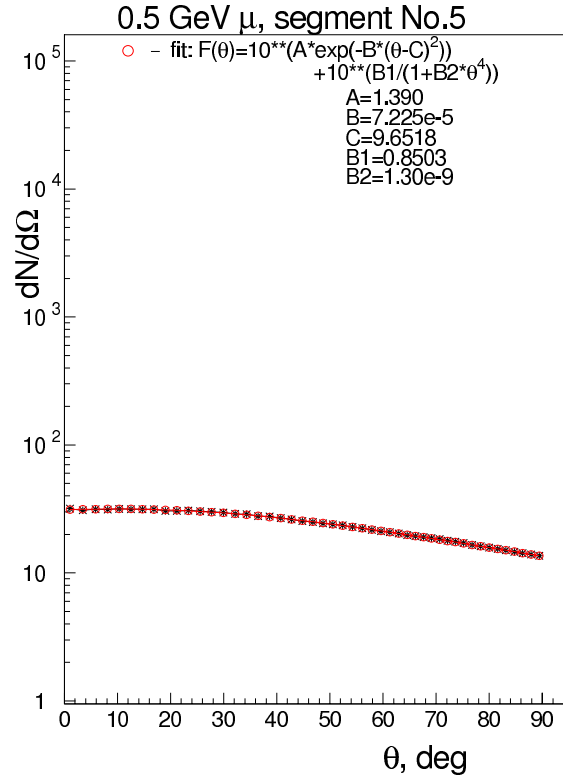


**Fig. 21.** fig:9e The angular structure function for 500 MeV muons from segment No.5. See the text for details.

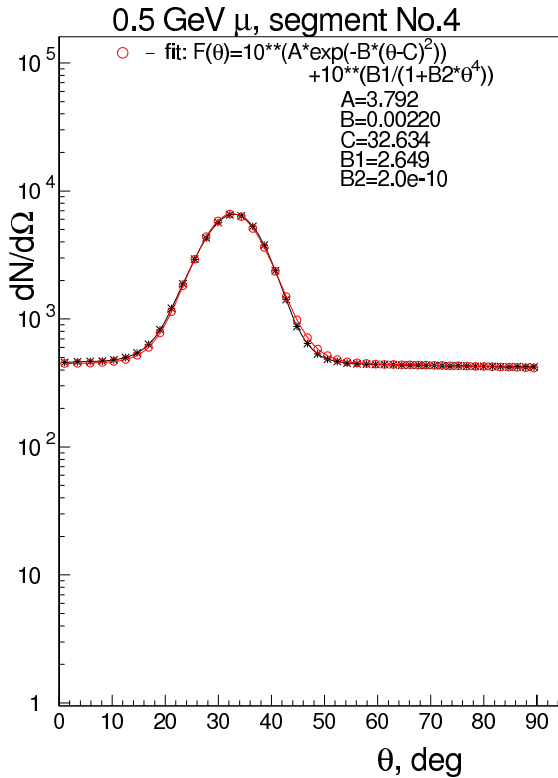


**Fig. 20.** fig:9d The angular structure function for 500 MeV muons from segment No.4. See the text for details.

side of the peak are from knock-on electrons and others with lower energies in the case of a muon. In the case of the electron initiated shower, the cascade of electrons with different energies and directions produces a broader spread of Cherenkov light. As the muon proceeds it loses energy, so that the angular distribution for the Cherenkov light becomes wider by multiple scattering while its mean value decreases due to the reduction of the Cherenkov angle. We can see this in Figures 18, 19 and 20, where the angular distributions change greatly between segments, while the production of Cherenkov light is maintained, which is a different characteristic from the corresponding curves in the case of the electron. In Figure 21, we find the disappearance of the peak of the angular distribution which was evident in the preceding segments. The uniformity of the distribution in Figure 21 shows that the decay electrons are distributed isotropically in this segment due to the nature of the three-body decay. According to the calculations on transition curves for the differential and integral Cherenkov photons, it is easily understood that there is no muon in segment No.5 (Fig.21) (160 cm to 200 cm from the starting point of the muon).

Also, we could not infer the starting point of the muon (the vertex point of muon neutrino interaction) from the edge of the Cherenkov ring, as adopted by the SK group, just as for the electron event. Comparing Figure 17 with Figures 18,19,20 the contributions from the segments No.2 (Fig.18), No.3 (Fig.19) and No.4 (Fig.20) near the edge of the Cherenkov ring are comparable with that from the

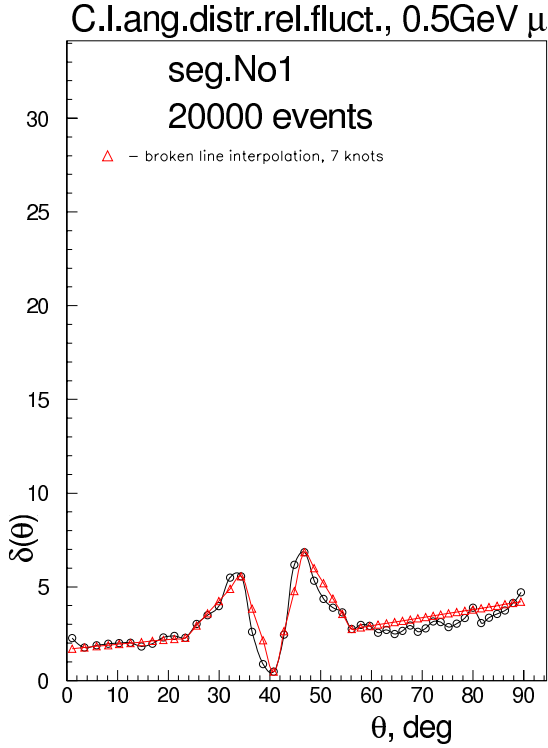


**Fig. 22.** fig:10a The relative fluctuations in the angular distribution of the Cherenkov light for 500 MeV muons from segment No.1. See the text for details.

segment No.1. In conclusion, we can determine the vertex point of the neutrino interaction, or the direction of the incident neutrino, based on the total pattern of Cherenkov light only, and not solely from the edge of the Cherenkov ring.

We can see that there is a clear difference in the relative fluctuations between the muon and electrons as well as that in the angular distribution functions. In Figures 22 to 25, there are peaks in the relative fluctuation either side of the local minimum at  $42^\circ$ . More exactly speaking, the strong concentration of the Cherenkov light around  $42^\circ$ , which is the consequence of the large contribution by the muon gives a deep minimum to fluctuation. The two peaks appear as the result of this, and the local minimum shifts to smaller angles, accompanied by the two peaks, as the muon proceeds, while there is only one peak in the case of an electron-initiated cascade.

However, in Figure 26 where the muon decays completely in the segment No.5 (160 cm to 200 cm from the starting point of the muon), the (decay product) electron is, on average, distributed uniformly and the distribution of the Cherenkov becomes uniform, so that the relative fluctuation also becomes uniform.

Comparing Figure 22 to 26 with Figure 12 to 16, it is easily understood that we could expect larger fluctuation in muon events than in electron events. The reasons are as follows: In electron events, the shower particles produced compensate for the effects of fluctuations, while in the muon events the single muon concerned bears the effect of the fluctuation exclusively due to multiple scattering,

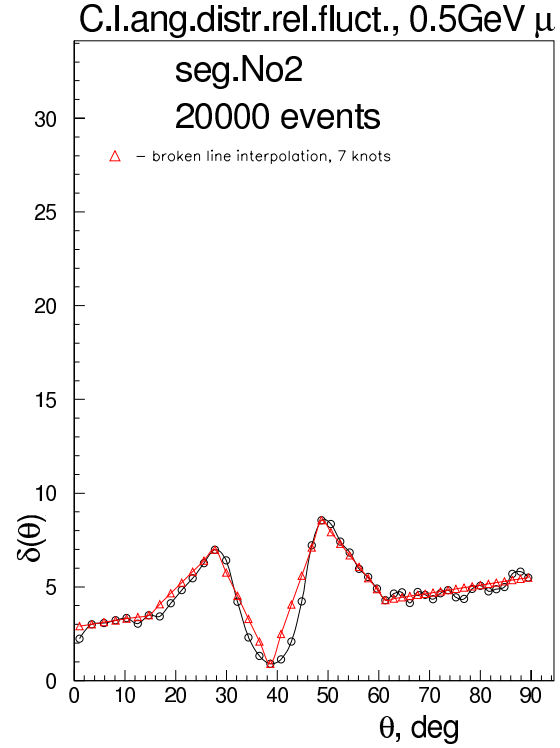


**Fig. 23.** fig:10b The relative fluctuations in the angular distribution of the Cherenkov light for 500 MeV muons from segment No.2. See the text for details.

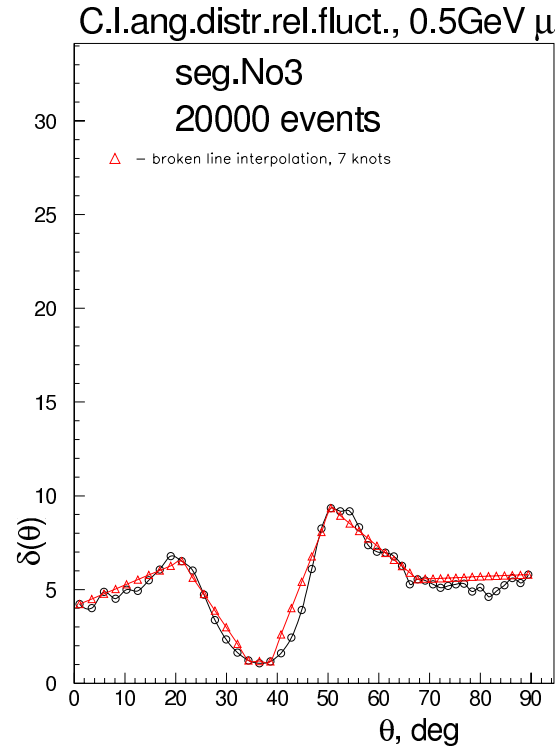


**Fig. 24.** fig:10c The relative fluctuations in the angular distribution of the Cherenkov light for 500 MeV muons from segment No.3. See the text for details.

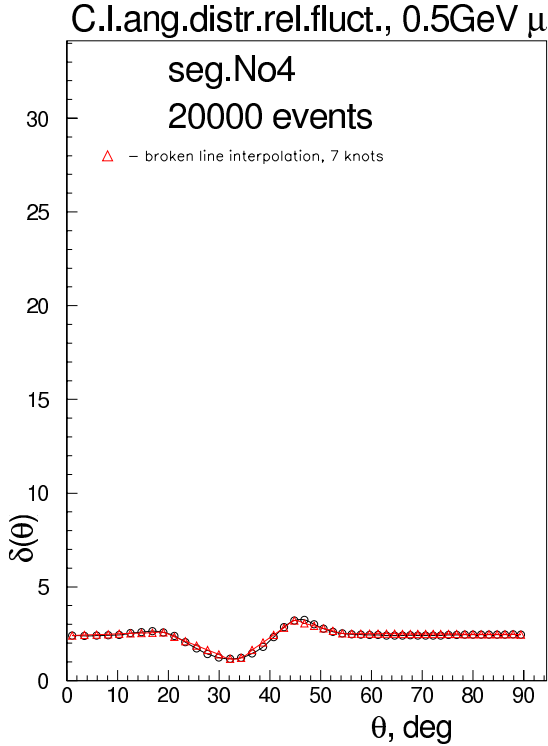


**Fig. 25.** fig:10d The relative fluctuations in the angular distribution of the Cherenkov light for 500 MeV muons from segment No.4. See the text for details.

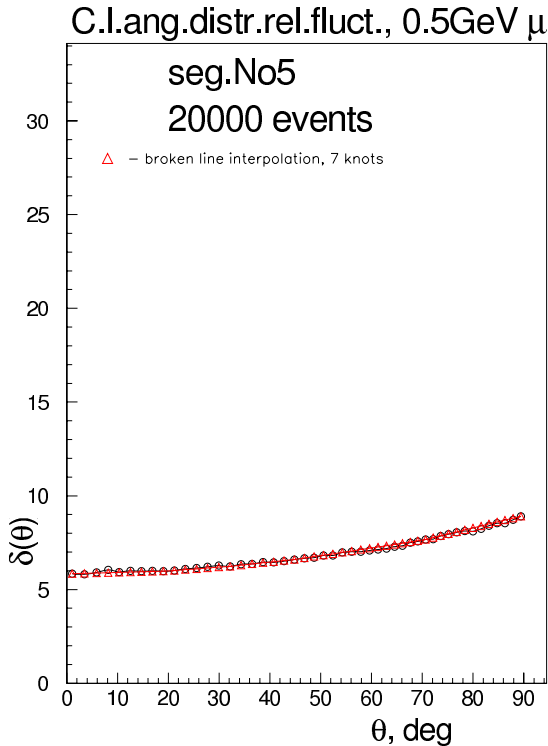


**Fig. 26.** fig:10e The relative fluctuations in the angular distribution of the Cherenkov light for 500 MeV muons from segment No.5. See the text for details.

which are not smeared out. As a result, we could expect a larger uncertainty in muon events for both the vertex position and the direction of the neutrino than in electron events. We discuss this problem in a subsequent paper.

## 4 Acknowledgement

One of the authors (V.G.) should like to thank Prof. M. Higuchi, Tohoku Gakuin University. Without his invitation, V.G. could not join in this work. Authors would like to be very grateful for the remarkable improvement of the manuscript to Dr. Philip Edwards.

## References

### 5 References

1. Kasuga *et al*, Phys.Lett.**B374**,(1996)238
2. Ashie *et al*,Phys.Rev.**D71**,(2005)112005
3. Ryazhskaya O.G., JETP.Lett.**60**,(1994)609  
Ryazhskaya O.G., JETP.Lett.**61**,(1995)229  
Khalchukov F.F*et al*, Nuovo Cimento **C18**,(1995)517  
Ryazhskaya O.G., Nuovo Cimento **C19**,(1996)655
4. Mitsui,K., Kitamura,T., Wada,T and Okei,K., J.Phys. G: Nucl.Part.Phys.**29**,(2003)2281
5. Kasuga,S., ICRR Report 338-95-4(1995)
6. Kasuga,S., Ph.D thesis, University of Tokyo(1998)
7. Sakai,A., Ph.D thesis, University of Tokyo(1997)
8. Kibayashi,A., Ph.D thesis, University of Hawaii (2002)
9. Takita,M., Ph.D thesis, University of Tokyo, (1988)
10. Ishitsuka,M., Ph.D Thesis, University of Tokyo (2004).
11. Kameda,J., Ph.D thesis, University of Tokyo (2002)
12. Okumura,K., Ph.D thesis, University of Tokyo (1999)
13. Messier,M.D., Ph.D thesis, Boston University (1999)